Available online at www.sciencedirect.com
SCIENCE DIRECT®
Atmospheric Environment 39 (2005) 3029–3038
ATMOSPHERIC ENVIRONMENT
www.elsevier.com/locate/atmosenv

Export of atmospheric mercury from Asia

Daniel Jaffe[a,*], Eric Prestbo[b], Phil Swartzendruber[a], Peter Weiss-Penzias[a], Shungo Kato[c], Akinori Takami[d], Shiro Hatakeyama[d], Yoshizumi Kajii[c]

[a]*Interdisciplinary Arts and Sciences, University of Washington-Bothell, Bothell, WA 98011 8246, USA*
[b]*Frontier Geosciences Inc. Seattle, WA, USA*
[c]*Applied Chemistry, Faculty of Engineering, Tokyo Metropolitan University, Tokyo, Japan*
[d]*Atmospheric Environmental Division, National Institute of Environmental Studies, Tsukuba, Japan*

Received 11 October 2004; accepted 2 January 2005

Abstract

Emissions inventories indicate that Asian Hg sources are more than 50% of the global anthropogenic total. However, few measurements have been made to verify these large emissions. In this paper, we report on measurements of mercury from two sites during spring 2004 which received Asian outflow: Hedo Station, Okinawa (HSO), Japan and the Mt. Bachelor Observatory (MBO) in central Oregon, USA. At both sites, export of atmospheric mercury from China and East Asia was verified by the observations and meteorological data. The mean Hg^0 concentration we observed at HSO was 2.04 ng m^{-3}, which is significantly higher than the global background. Measurements of reactive gaseous mercury and particulate mercury at HSO found relatively little outflow of these compounds from Asia, generally less than 3% of the total mercury. By examining the correlation of Hg^0 to carbon monoxide during outflow events, we have derived an enhancement ratio, which should reflect the ratio of these compounds in the source region. During outflow from Asia, the mean Hg^0/CO molar enhancement ratio we observed at HSO was 6.2×10^{-7}, which is nearly twice the expected ratio based on emissions estimates from China. During one episode of long-range transport from Asia to the MBO, we found a very similar ratio of Hg^0/CO to that observed at HSO and a similar ratio was also reported by Friedli et al. (2004, Journal of Geophysical Research 109, D19 S25) downwind of Shanghai. Thus the ratio of Hg^0/CO appears to be a good tracer of Asian industrial outflow. Using the Hg^0/CO ratio and a recent inventory for CO emissions, we calculate Hg^0 emissions from Asia of 1460 metric tons $year^{-1}$, which is nearly two times the value in the Pacyna et al. (2003, Global mercury emissions. Presented at Long-Range Transport Workshop, Ann Arbor, MI, September 2003) inventory. Several hypotheses are proposed to explain this discrepancy, including an underestimation of the Chinese industrial Hg^0 emissions, natural sources, significant re-emissions of previously deposited Hg and/or a higher ratio of Hg^0/total Hg in the outflow from Asia than in the emission inventory.

Keywords: Mercury; Asia; Emissions; Carbon monoxide

1. Introduction

Mercury is a powerful neurotoxin, especially in its methylated forms, and can bio-accumulate, leading to dangerous concentrations in some species of fish.

*Corresponding author. Tel.: +1 425 352 5357; fax: +1 425 352 5233.
E-mail address: djaffe@u.washington.edu (D. Jaffe).

1352-2310/$ - see front matter © 2005 Elsevier Ltd. All rights reserved.
doi:10.1016/j.atmosenv.2005.01.030

Advisories to limit consumption of high-mercury fish species have been issued in many countries and in 48 states of the US. However, quantifying the source of this mercury is difficult due to mercury's complex bio-geo-atmospheric cycling (US EPA, 1997).

Mercury is released largely in the elemental form, but there are also significant emissions of particulate and oxidized Hg^{2+} (Prestbo and Bloom, 1995; Carpi, 1997; Lin and Pehkonen, 1999; Schroeder and Munthe, 1998). The lifetime of the elemental form is between 6 and 24 months (Weiss-Penzias et al., 2003), which means that it can be transported globally. The lifetime of the particulate and the oxidized forms is on the order of a day or week (Schroeder and Munthe, 1998), which means that these species are largely deposited locally, close to the source. Global atmospheric emissions of mercury in 1995 from industrial activities are around 2400 tons $year^{-1}$, 53% as Hg^0, 37% as gaseous Hg^{2+} and the remainder as particulate-bound Hg (Pacyna and Pacyna, 2002). In developed countries, emissions of mercury appear to be decreasing, due to emission controls on other pollutants (Mukherjee et al., 2000; US EPA, 1997). Globally, however, it appears that mercury emissions and Hg^0 concentrations are still increasing (Fitzgerald, 1995; Slemr and Langer, 1992), in part due to the rapidly expanding economies of East Asia and the large amount of coal that is burned in the region (Kim and Kim, 2000; Tan et al., 2000). The emissions from Asia are about 56% of the global anthropogenic emissions (Pacyna and Pacyna, 2002; Pacyna et al., 2003). In one global modeling study, Asian emissions are estimated to contribute between 5% and 36% of total mercury deposition in the US (Seigneur et al., 2004). Additionally, re-emission of previously deposited anthropogenic mercury results in a significant, but poorly quantified, fraction of the atmospheric Hg^0 burden (Mason et al., 1994). The sum of current emissions plus re-emissions has resulted in an increase of the total deposition of anthropogenic mercury by a factor of 3–20, since pre-industrial times (Bergan et al., 1999; Schuster et al., 2002).

Because of the large Asian emissions of Hg and the frequent occurrence of long-range transport of pollutants from Asia to North America (Jaffe et al., 1999, 2001, 2003; Price et al., 2004; Weiss-Penzias et al., 2004), we set out to better define the Asian emissions of Hg and to see whether long-range transport of Hg could be identified. To this end, during spring 2004, we made simultaneous observations at two sites: Hedo Station, Okinawa (HSO) and the Mt. Bachelor Observatory (MBO) in central Oregon. At both sites, transport of atmospheric mercury from Asia was clearly identified. In this report, we will focus on the Hg and CO observations and use these to constrain the Asian emissions, quantify the mercury speciation in the Asian outflow and to better understand the long-range transport of mercury to North America. In future publications, we will report on additional observations made at HSO and MBO, focusing on the factors controlling reactive gaseous and particulate Hg as well as long-range transport (Prestbo et al., Observations of atmospheric mercury species at Cape Hedo, Okinawa, manuscript in preparation; Weiss-Penzias et al., Observations of CO, ozone, aerosols and total gaseous mercury (TGM) in Asian pollution plumes at MBO during Spring 2004, manuscript in preparation).

2. Experimental

The Hedo station is located on the north end of the island of Okinawa (26.8N, 128.2E, 60 m a.s.l.), away from the island's major population centers. This site has been used for a number of years to study the outflow of pollution from East Asia and China (Kato et al., 2004; Kanaya et al., 2001). At HSO, we measured Hg^0, reactive gaseous mercury (RGM) and fine ($<2.5\,\mu m$) particulate-bound Hg (PHg). Measurements were made from 23 March to 2 May 2004. This supplemented the on-going measurements of CO, O_3, aerosol scattering and chemistry, SO_2, NO_x and meteorology. For this work, we will use only the Hg and CO data. Other observations will be reported in subsequent publications (Prestbo et al., manuscript in preparation).

At HSO, we measured Hg^0, RGM and PHg using a continuous, species-selective, pre-concentration system coupled to a cold vapor atomic fluorescence spectroscopy (CVAFS) detector (Tekran 2537/1130/1135, see Landis et al., 2002). Air was sampled at $10\,l\,min^{-1}$ through a fine-particle impactor ($2.5\,\mu m$) to exclude the coarse aerosol, followed by a KCl-coated annular denuder to selectively adsorb the RGM species and then a quartz particulate filter to capture the particulate-bound mercury. The entire impactor–denuder–filter apparatus and sample lines were held at 50 °C during sampling. Elemental mercury passes through the impactor–denuder–filter apparatus and a slipstream of $1.0\,l\,min^{-1}$ was sampled by the CVAFS detector, with the remaining $9\,l\,min^{-1}$ vented to the air. The CVAFS instrument pre-concentrates and separates the Hg^0 from the air matrix by capturing it on a gold cartridge for 5 min. The mercury amalgamated to the gold is then thermally desorbed and detected by the atomic fluorescence detector. The instrument contains two matched gold traps, which allow for continuous integrated measurements via alternating sampling and detection. After 3 h, the automated system was programmed to stop sampling through the impactor–denuder–filter apparatus, while the CVAFS detector continues to sample. Simultaneously, the zero air is supplied to the inlet via a pump and impregnated carbon filter system. After measuring the zero air blanks, the particulate filter

is heated in zero air to 650 °C followed by heating the annular denuder to 500 °C. The thermal desorption step converts all the mercury on the quartz filter and annular denuder to the Hg^0 form, for detection by the CVAFS (Landis et al., 2002). The result is 3 h of continuous Hg^0 data in 5-min intervals and a single, integrated RGM and PHg value over the same period. During the 1-h RGM and PHg desorb period, no Hg^0 sampling occurs. The automated CVAFS instrument has proven itself by operating unattended for long periods under severe atmospheric conditions at Mace Head, Ireland, Alert, Canada and Cheeka Peak, Washington (Ebinghaus et al., 1999; Schroeder et al., 1998; Weiss-Penzias et al., 2003).

The CVAFS detector was automatically calibrated every 40 h using an internal elemental mercury permeation source held at 50 ± 0.1 °C. The calibration consists of a zero and span at approximately 10 times normal concentration, for each gold cartridge. The internal source was calibrated against a primary standard of saturated Hg^0 held at a known and highly precise temperature (± 0.002 °C, Tekran 2505, see Landis et al., 2002).

Over the course of the campaign, the precision of the automatic calibrations using the permeation source was 1.1% (1σ). The 1-σ precision of the Hg^0 measurements is estimated to be 2% based on replicate observations during stable periods. The accuracy of the Hg^0 concentrations is estimated to be 11% based on a propagation of errors method. The total Hg^0 uncertainty is 12%. Since the RGM and PHg are detected as Hg^0, their precision and accuracy are no better than those for Hg^0. Based on laboratory studies, the 1-σ precision at the pg m^{-3} level for RGM and PHg is approximately 15% (Landis et al., 2002). Currently, there are no calibration standards for RGM and PHg.

At HSO, carbon monoxide was measured using a non-dispersive infrared instrument (Themo Environmental Instruments Model 48C). The instrument samples ambient air for 45 min and zero air for 15 min each hour. Zero air was generated from ambient air using a heated platinum catalyst (TEI Model 96) to remove CO. This maintains water vapor in the zero air at nearly the same level as ambient. Calibration gas (1.8 ppmv Nippon-sanso) was introduced regularly to monitor the instrument sensitivity, which proved to be very stable. The measurement uncertainty was 8 ppbv or 6%, whichever is greater.

MBO is a new site located on the summit of an extinct volcano in central Oregon, USA (43.98°N 121.69°W 2.7 km a.s.l.). The atmospheric research site was established in 2004 with the cooperation of the Mt. Bachelor Ski Area. The sampling site is located on the roof of the summit building, which likely experiences free tropospheric air a large fraction of the time. During spring 2004, we measured CO, O_3, aerosol scatter, NO_x and total mercury. For this work, we focus on the Hg and CO data, which are described below. Consistent with our previous work, we use short-lived tracers, such as NO_x, to help identify local pollution. Other observations will be reported in subsequent publications (Weiss-Penzias et al., manuscript in preparation).

The MBO summit elevation of 2.7 km results in an average pressure of around 730 mbar. At this height, the flow is predominantly from the southwest through northwesterly directions. The site is approximately 180 km east of the Pacific coast. While there are some small cities and one major highway to the west of MBO, these are much lower in elevation. During the spring observations, we have not been able to identify influence from these local sources. While it is still possible that there is some influence from these nearby sources, it is likely that their influence is minimal.

At MBO, total Hg was measured using a Tekran 2537A, similar to HSO. While we expect that most of the atmospheric mercury at MBO is in the Hg^0, the presence of PHg and RGM can create significant artifacts if the sampling technique is not properly designed (Landis et al., 2002). We therefore elected to quantify total mercury (THg), which is the sum of Hg^0, RGM and PHg. The inlet consisted of a quartz tube wrapped with a heating element, which was held above 130 °C. The conversion of RGM and PHg to elemental Hg was carried out in a pyrolyzer located immediately after the inlet. This consisted of a quartz tube packed with quartz chips, maintained at 500 °C in a tube furnace.

The 2537A was configured to sample on a 5 min collection cycle with a flow rate of 0.75 slpm. This yielded a 3-σ method detection limit of 0.06 ng m^{-3}. The instrument automatically calibrated to an internal permeation source every 18 h and the accuracy of the factory-specified permeation rate was compared against manual injections of a primary vapor source (Tekran model 2505). The two calibration methods agreed to better than 6%. The hourly precision was 1% and the mean precision of successive internal calibrations was better than 1%. Before, during and after deployment in the field, the blank level of the front-end system (i.e. the sample line, pyrolyzer, and heated inlet) was measured by connecting a mercury scrubbing iodated carbon trap. All of these blank measurements revealed a non-detectable or negligible contribution to the signal.

At MBO, CO was measured using a non-dispersive infrared instrument (Thermo-Electron Corp., Model 48C). This is the same type of instrument used at HSO, although there were some differences in the operating procedures. Ambient air and CO-scrubbed ambient air (passed through a heated catalyst) were alternately sampled on a 10-min switching schedule. This allowed for accurate determination of the instrument's zero level, which is prone to drifting due to pressure and temperature variations. Calibrations were

performed once daily with bottled breathing air containing approximately 500 ppbv CO. The final CO value in the working standard was referenced to a NIST CO standard (9.75 ppm) before and after the spring campaign. The accuracy of our measurements based on cross-referencing with other standards over a 3-year period is better than 5%. The method detection limit was found to be 21 ppbv based on 3 times the standard deviation of repetitive zero measurements. At levels above the detection limit, we estimate the uncertainty in the reported hourly averages to be 6%.

We calculated kinematic back-trajectories using the NOAA-HYSPLIT model (Draxler and Rolph, 2003). For the trajectory calculations we used the NCEP-FNL meteorological dataset, which has a time resolution of 6 h and a horizontal resolution of $1^\circ \times 1^\circ$. All mercury data are reported in ng or pg per standard cubic meter, which is important since data from several altitudes are reported. All HSO and MBO data are reduced to hourly averages for the statistical calculations and presentations reported in this paper.

3. Theoretical considerations

To analyze the results and calculate the emissions of Hg^0, we use the observed ratios of CO and Hg during plume encounters. Numerous researchers have used the ratio of two or more compounds measured in ambient air as a tool to provide quantitative information on the emission strengths. The method described below is largely based on work presented by Hansen et al. (1989) and used by other researchers (e.g. Jaffe et al., 1995; Carmichael et al., 2003). This method relies on the fact that the ratio of two compounds released from a common source will be maintained during mixing and dilution, provided certain assumptions are true.

Consider two compounds X and Y:

$$\mathrm{ER} = Y_0/X_0, \tag{1}$$

$$Y_{\mathrm{amb}} = Y_{\mathrm{bg}} + KY_0, \tag{2}$$

$$X_{\mathrm{amb}} = X_{\mathrm{bg}} + KX_0, \tag{3}$$

where ER is the emission ratio at the source, Y_0 and X_0 are the concentrations of Y and X at the source, Y_{bg} and X_{bg} are the background concentrations and Y_{amb} and X_{amb} are the ambient concentrations following mixing and dilution. K is a variable which represents the degree of dilution, which is the same for both X and Y.

Re-arranging and eliminating K, we get

$$Y_{\mathrm{amb}} = X_{\mathrm{amb}} Y_0/X_0 + \mathrm{constant}. \tag{4}$$

In other words, a plot of Y_{amb} vs. X_{amb} during a plume encounter will yield a straight line with a slope equal to the emissions ratio. This assumes:

(1) No chemical or physical loss, only dilution;
(2) Constant emission source with fixed Y_0/X_0 ratio;
(3) Constant background concentrations.

If the emission flux of either compound is known, then the emissions of the second compound can be calculated by

$$F_y = F_x \mathrm{ER}, \tag{5}$$

where F_y and F_x are the emission fluxes for compounds Y and X, respectively.

To the extent that a plot of Y_{amb} vs. X_{amb} shows a good linear relationship, our assumptions are valid. If there are multiple sources or changing backgrounds, the X–Y scatterplot will not yield a good correlation coefficient. For our analysis, we use CO and Hg^0 for X and Y, respectively, since an emission inventory of CO from Asia is available, and this inventory has been extensively evaluated against atmospheric observations (Palmer et al., 2003; Kasibhatla et al., 2002). In addition, both CO and Hg^0 have lifetimes that are much longer than the transit time across the Pacific, which is typically around 6–10 days.

4. Results

Table 1 provides a statistical overview of the observations at both HSO and MBO.

Mean Hg^0 concentrations at MBO are close to the global background at that latitude. HSO mean concentrations reflect a significant enhancement over the global background, consistent with the prevailing westerly flow to the station from continental Asia. Fig. 1 shows a time series of the observations of CO, Hg^0 and PHg from

Table 1
Summary of Hg and CO observations at Hedo Station Okinawa (HSO, 23 March–2 May 2004) and the Mt. bachelor observatory (MBO, 28 March–17 May 2004)

HSO	Hg^0 ($ng\,m^{-3}$)	RGM ($pg\,m^{-3}$)	PHg ($pg\,m^{-3}$)	CO (ppbv)
Mean	2.04	4.51	3.04	215
Median	1.99	2.50	2.36	200
Min	1.37	0.12	0.10	98
Max	4.74	32.5	16.4	761
MBO[*]				
Mean	1.77	n.d.	n.d.	167
Median	1.76	n.d.	n.d.	169
Min	1.47	n.d.	n.d.	109
Max	2.51	n.d.	n.d.	296

[*]MBO data is for total Hg.

HSO. A number of periods with significantly enhanced Hg^0 and CO are apparent. During some of these episodes, PHg is also somewhat enhanced, although the concentrations never exceed 16 pg m^{-3}. Overall, CO and Hg^0 show excellent correlation during this campaign (see Table 2). PHg is moderately correlated with both CO and Hg^0 (significant at greater than 99% confidence). RGM is not correlated with any other species, but is correlated with the solar flux (discussed in Prestbo et al., manuscript in preparation). A scatterplot of Hg^0 vs. CO plot (Fig. 2) shows this strong correlation, yielding a slope of 0.0053 ng m^{-3} ppbv^{-1}. As discussed below, this slope appears to be characteristic of the Asian outflow and provides important information on the relationship of these two species in the source region.

From Fig. 1, we can identify a number of pollution transport episodes to HSO. Here we focus on the largest of these, labeled 1–6 in Fig. 1. Details on these six episodes are given in Table 3. Using the HYSPLIT back-trajectories, we can determine the most likely source region for each episode. For example, Fig. 3 shows the trajectory for 20 April 2004, GMT hour 0 (doy 111.0), which is near the beginning of episode #5. Fig. 3 shows that this airmass subsided over China from 3 and 4 km altitude and reached the boundary layer near the Chinese coast as it continued on to Okinawa. We should point out that trajectories only give a general indication of the source region and, in particular, are less accurate in identifying vertical motions. Thus it is not surprising that the complex boundary layer-free tropospheric exchange process is not modeled well by trajectories. Nonetheless, we feel that identification of continental Asian sources at HSO using trajectories is justified for these episodes. For episode 5, trajectories for the entire period are similar to Fig. 3, and indicate that emissions from China are the most probable cause of the high CO and Hg concentrations we observed.

While the trajectories from episodes 2 and 5 suggest predominantly Chinese emissions sources, the trajectories for episodes 1, 3, 4 and 6 indicate flow from China

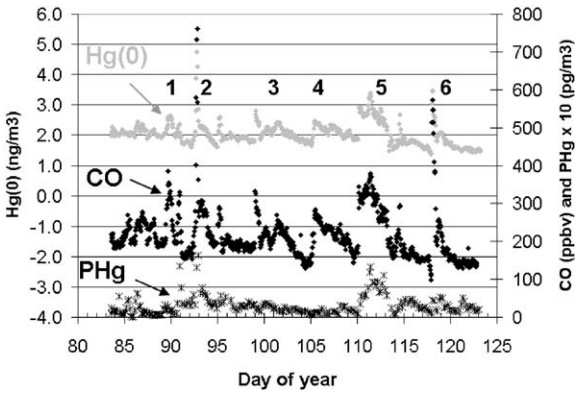

Fig. 1. Observations of CO (ppbv), Hg^0 (ng m^{-3}) and PHg (pg m^{-3}) at Hedo Station during spring 2004. Note that the PHg data are multiplied by 10 and plotted on the right axis. The numbers refer to event numbers, described in the text.

Table 2
Correlation coefficient (R^2) for various relationships using all data taken at HSO

	CO	Hg^0	RGM	PHg
CO	***	0.84	0.01	0.25
Hg^0	***	***	0.04	0.24

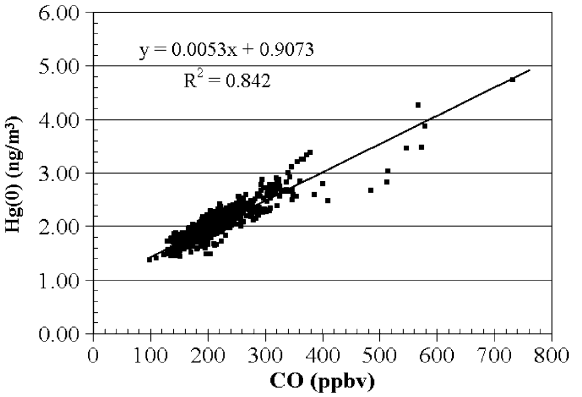

Fig. 2. Scatterplot of Hg^0 vs. CO for all Okinawa data.

Table 3
Correlation of HSO and MBO data for specific episodes (see Fig. 1)

Event #	DOY	Hg^0 vs. CO ng m^{-3} ppbv^{-1}	R^2	Source region (Hysplit)
HSO #1	89.1–91.8	0.0043	0.87	China/E. Asia
HSO #2	92.1–94.8	0.0056	0.98	China
HSO #3	98.63–99.7	0.0073	0.99	China/Korea
HSO #4	104.5–107.7	0.0051	0.78	China/E. Asia
HSO #5	109.9–114.1	0.0074	0.90	China
HSO #6	117.9–119.7	0.0036	0.93	China/Korea
HSO mean $\pm 1\sigma$	0.0056 ± 0.0016			
MBO #1	115.7–117.9	0.0050	0.92	E.Asia

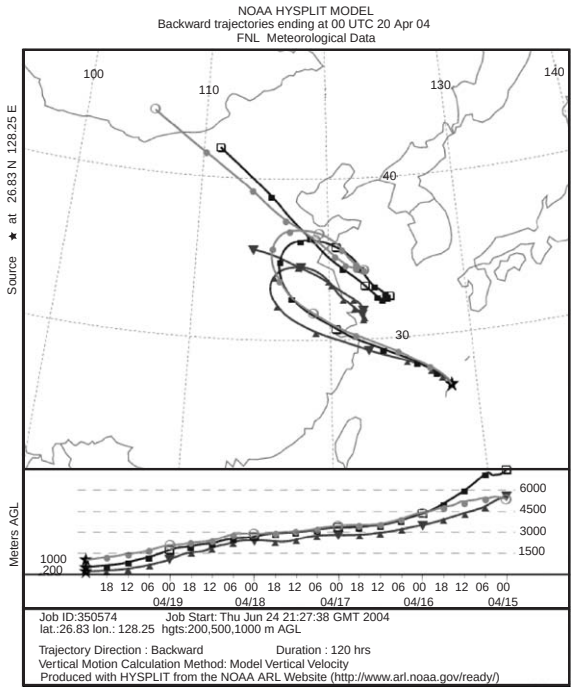

Fig. 3. NOAA-HYSPLIT back-trajectory for HSO Event ♯5.

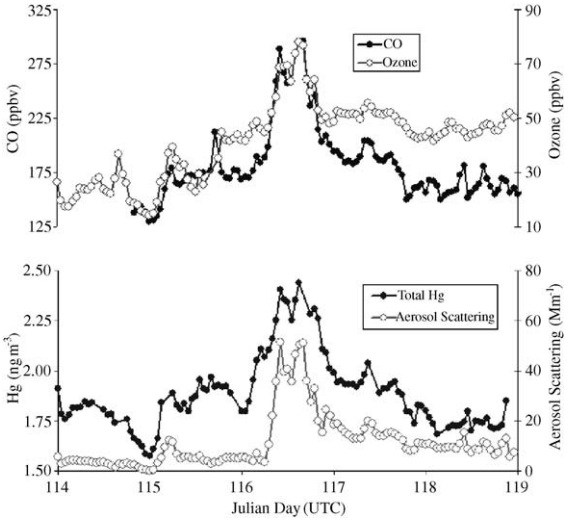

Fig. 4. Observations of CO (ppbv), O_3 (ppbv), aerosol scattering (Mm^{-1}) and total Hg ($ng\,m^{-3}$) at MBO from 23 to 28 April 2004 (DOY 114–119).

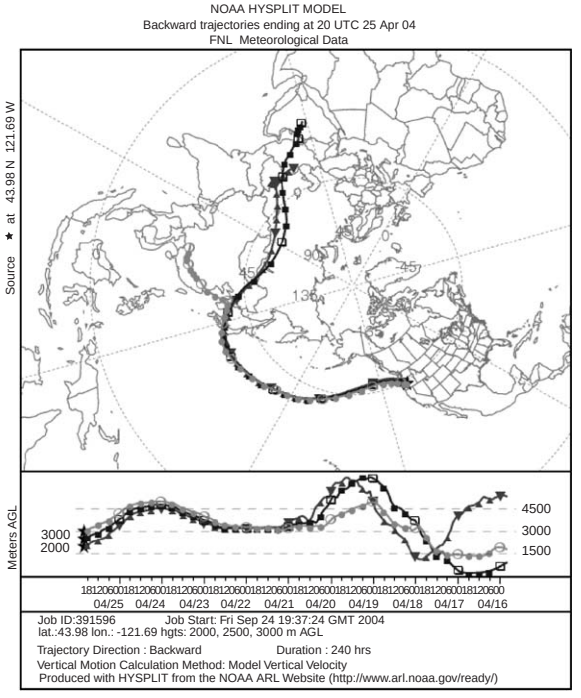

Fig. 5. NOAA-HYSPLIT back-trajectory for MBO episode on 25 April 2004.

and other industrial regions in East Asia as well. For each episode identified in Table 3, we found a good linear relationship between Hg^0 and CO. The slopes and R^2 for each episode are given in Table 3. It should come as no surprise that the mean slope of these six episodes ($0.0056\,ng\,m^{-3}\,ppbv^{-1}$) is nearly the same as the slope for the entire campaign ($.0053\,ng\,m^{-3}\,ppbv^{-1}$). However despite this, there are variations in this slope (s.d. $= 0.0016\,ng\,m^{-3} - ppbv^{-1}$). We interpret these variations as reflecting variations in the dominant source regions for each episode.

During outflow events observed at HSO, RGM and PHg were usually only slightly enhanced. The largest enhancement we found was for event ♯5, when RGM + PHg made up 3% of the total Hg enhancement. This low value likely reflects the rapid removal of RGM and PHg during transport in the marine boundary layer to HSO. Friedli et al. (2004) found that 12.5% of the Hg was in the form of PHg for the Shanghai plume. This is significantly greater than the values we found, probably reflecting a longer lifetime for PHg above the boundary layer. Further analysis of the HSO RGM and PHg data is found in Prestbo et al. (manuscript in preparation).

At MBO, we identified several long-range transport episodes, which took place during spring 2004 (Weiss et al., manuscript in preparation). Here we will focus on the largest episode, which occurred on 25 April 2004. Fig. 4 shows a time series of data from MBO for this period. Fig. 5 shows a HYSPLIT back trajectory for 25 April at several elevations above and below the site elevation. We also calculated back-trajectories for the same date on the corners of a $1^\circ \times 1^\circ$ box around the site location and at multiple elevations. In all cases, the trajectories showed similar flow, which indicates

transport of a relatively coherent airmass. While the MBO site at 2.7 km a.s.l. generally sees little influence from nearby boundary-layer pollution sources, it is possible that local pollutants could have contributed to the episode seen on 25 April 2004. For this reason, we use short-lived tracer to indicate possible contributions from nearby emission sources. From our previous work, we have found that NO_x, which has a lifetime of about 1 day or less, is strongly enhanced during local pollution episodes, but not enhanced at all during long-range transport events (Jaffe et al., 1999, 2001). For this reason, NO_x measurements are conducted routinely at MBO. During the period shown in Fig. 4, NO_x measurements were very low, uncorrelated with the other tracers and rarely above their detection limit. In addition, the back-trajectories for 25 April do not suggest any contribution from nearby boundary layer sources. Taken together, the chemical and meteorological data indicate that local emissions are not the cause of the enhancements seen on 25 April.

The nature of this long-range transport episode is similar to previous Asian long-range transport episodes that we have identified from our aircraft data (Kotchenruther et al., 2001; Bertschi et al., 2004; Price et al., 2004a). For example, the CO enhancement for the 25 April 2004 episode was 145 ppbv, compared to enhancements of 15–140 ppbv for other Asian LRT episodes we have identified in the free troposphere by aircraft (Bertschi et al., 2004; Price et al., 2004b). This LRT episode was also significantly larger than any we have seen in the marine boundary layer (e.g. Jaffe et al., 1999, 2001), which have CO enhancements in the range of 22–32 ppbv. Based on the trajectories and the similarity with our previous observations of LRT, we are confident that the 25 April 2004 episode was due to Asian emission sources.

For the 25 April LRT episode at MBO, CO and Hg^0 showed excellent correlation. Table 3 shows the slope and correlation coefficient for this event. It is important to note that the slope for this episode is very similar to the slopes seen at HSO. The implications of this are discussed below.

5. Discussion

There has been one previous observation of mercury outflow from Asia (Friedli et al., 2004). In this report, observations of Hg^0 and RGM were made by aircraft downwind of Asia during the 2001 ACE-Asia field experiment. The mean TGM concentration observed by Friedli et al. (2004) in the marine boundary layer downwind of Asia was approximately 2.1 ng m^{-3}, very similar to our mean value at HSO (Table 1). During one encounter of the Shanghai plume, Friedli et al. (2004) reported a TGM/CO ratio of 6.4×10^{-6} on a w/w basis. This converts to a Hg^0/CO ratio of 0.0056 ng m^{-3} ppbv^{-1}, virtually identical to the slope we observed for all data at HSO, the mean slope for the six HSO episodes shown in Table 2 and the ratio from the one MBO episode. Based on the measured Hg^0/CO ratio reported here for HSO (0.0056 ng m^{-3} ppbv^{-1}), MBO (0.0050 ng m^{-3} ppbv^{-1}) and the observations of Friedli et al. (0.0056 ng m^{-3} ppbv^{-1}), this ratio appears to be characteristic of Asian outflow. Converting this to a molar ratio, the mean slope for the six HSO events (Table 3) is 6.2×10^{-7} ($\pm 1.7 \times 10^{-7}$, 1σ).

Based on Eq. (4), this ratio should reflect the emission ratio for CO and Hg^0 from Asia. Table 4 provides information on industrial Hg emissions for Asia, China, as well as other regions of the Northern Hemisphere. Also shown are the combined fuel combustion emissions of CO. This includes combustion of fossil fuels and biofuels, which are thought to make an important contribution to total CO emissions in Asia. The CO emissions in Table 4 do not include biomass burning, which is highly episodic. The Asian Hg/CO ratio is the highest in the Northern Hemisphere, which largely reflects the dominant role of coal for power generation. It is interesting to note that the ratio for the west coast of the US (Washington, Oregon and California) is lower by a factor of ~20. This suggests that the Hg/CO ratio may be a useful tool to identify Asian pollution at MBO, and other west coast observatories.

Using Eq. (4), the observed molar Hg^0/CO ratio of 6.2×10^{-7} and the CO emissions from Table 4, we calculate Hg^0 emissions from Asia of 1460 metric tons year^{-1}, which is substantially larger than the industrial Hg^0 emissions of 770 metric tons year^{-1} from the Pacyna et al. (2003) inventory. By propagation of error based on the measurement uncertainties and the uncertainty in the CO inventory (~25%), we estimate the uncertainty in our calculated Asian emissions at ±30%. So even considering this uncertainty, there remains a significant discrepancy between our calculated Asian Hg^0 emissions and the emission inventory of Pacyna et al. (2003). It is possible that the CO inventory has larger errors; however, we considered this unlikely due to the extensive validation that has been conducted for the CO emissions from Asia (Palmer et al., 2003; Heald et al., 2003, 2004). Note that while European and North American sources likely contribute to the background Hg^0 concentrations, these are not significant contributors to the plume enhancements seen at HSO, MBO and the data reported by Friedli et al. (2004).

There are several possible explanations for the discrepancy in Asian Hg^0 emissions described above:

(1) The Asian industrial Hg^0 emissions are too low. Note that for CO it was found that residential coal and biofuel consumption made a large contribution

Table 4
Emissions of CO and Hg^0 for various regions of the globe (metric tons $year^{-1}$)

Region	CO emissions ($\times 10^6$ metric tons $year^{-1}$)	Total Hg emissions (metric tons $year^{-1}$)	Hg^0 emissions (metric tons $year^{-1}$)	Tot Hg/CO (molar)	Hg^0/CO (molar)	Data sources
Washington (state)	1.86	0.22	0.12	1.6×10^{-8}	8.5×10^{-9}	1,2
Oregon	1.82	0.24	0.13	1.8×10^{-8}	9.4×10^{-9}	1,2
California	7.35	2.6	1.37	4.8×10^{-8}	2.5×10^{-8}	1,2
North America	156	202	129	1.8×10^{-7}	1.1×10^{-7}	3,4
Europe	100	239	152	3.2×10^{-7}	2.1×10^{-7}	3,4
Asia	328	1204	770	5.0×10^{-7}	3.2×10^{-7}	3,4
China	168	604	387	4.9×10^{-7}	3.1×10^{-7}	3,4

1. Hg data from US environmental protection agency, toxic release inventory. Available online at: http://www.epa.gov/tri/.
2. CO data for 1998 from USEPA, 2000.
3. Hg data for the year 2000 from Pacyna et al. (2003).
4. For all countries except China, CO data are from the GEIA EDGAR emissions inventory, version 3.2. Available online at: http://gaiacenter.org. For China, we used CO data for 2001 from Palmer et al. (2003).

to the total emissions and this was underestimated in early emission inventories (Palmer et al., 2003; Kasibhatla et al., 2002).
(2) Re-emission of previously deposited Hg makes a substantial contribution to the total emissions.
(3) Natural emissions make a substantial contribution to the total emissions.
(4) The fraction of Hg^0/total Hg in the emissions inventory is underestimated. Pacyna et al. (2003) used a value of 64%, which could be low. Note that our estimated Asian Hg^0 emissions (1460 metric tons $year^{-1}$) is much closer to the Pacyna et al. (2003) emissions for total Hg (1204 metric tons $year^{-1}$).
(5) Conversion of RGM and/or PHg to Hg^0 occurs in the stack or in the plume during transit (Prestbo et al., 2004).

Our data confirm that Asia is a large source of Hg to the global atmosphere. Based on observations from three different platforms (HSO, MBO and aircraft) by two different groups (this work and Friedli et al., 2004) the Hg/CO ratio is a good tracer of Asian airmasses. However, there are clearly important aspects of the Asian emissions that we do not understand well. Most importantly, there appears to be a substantial discrepancy between the Hg emissions in the Pacyna et al. (2003) inventory and calculated emissions based on observations. We have proposed several possible hypotheses to explain these discrepancies, but our data do not allow us to identify the exact cause. Clearly, it is important to better understand the Hg emissions and outflow from Asia. Combining these and future observations with chemical transport models of mercury (e.g. Seigneur et al., 2004) should provide important new insights into the global flux and deposition of Hg.

Acknowledgements

We gratefully acknowledge the assistance of scientists and staff from Oregon State University and the Mt. Bachelor Ski Area. The research described in the article has been funded by the US Environmental Protection Agency's STAR program. It has not been subjected to any EPA review and therefore does not necessarily reflect the views of the Agency.

References

Bergan, T., Gallardo, L., Rodhe, H., 1999. Mercury in the global troposphere: a three dimensional model study. Atmospheric Environment 33, 1575–1585.

Bertschi, I.B., Jaffe, D.A., Jaeglé, L., Price, H.U., Dennison, J.B., 2004. PHOBEA/ITCT 2002 airborne observations of trans-Pacific transport of ozone, CO, VOCs and aerosols to the northeast Pacific: impacts of Asian anthropogenic and Siberian Boreal fire emissions. Journal of Geophysical Research 109 (D23), D23S12.

Carmichael, G.R., et al., 2003. Evaluating regional emission estimates using the TRACE-P observations. Journal of Geophysical Research 108 (D21), 8810.

Carpi, A., 1997. Mercury from combustion sources: a review of the chemical species emitted and their transport in the atmosphere. Water, Air and Soil Pollution 98, 241–254.

Draxler, R.R., Rolph, G.D., 2003. HYSPLIT (HYbrid Single-Particle Lagrangian Integrated Trajectory). Model access via NOAA ARL READY Website http://www.arl.noaa.gov/ready/hysplit4.html, NOAA Air Resources Laboratory, Silver Spring, MD.

Ebinghaus, R., et al., 1999. International field intercomparison measurements of atmospheric mercury species at Mace Head, Ireland. Atmospheric Environment 33, 3063.

Fitzgerald, W.F., 1995. Is mercury increasing in the atmosphere? The need for an atmospheric mercury network (AMNET). Water, Air and Soil Pollution 80, 245–254.

Friedli, H.R., Radke, L.F., Prescott, R., Li, P., Woo, J.-H., Carmichael, G.R., 2004. Mercury in the atmosphere around Japan, Korea and China as observed during the 2001 ACE-Asia field campaign: measurements, distributions, sources, and implications. Journal of Geophysical Research 109, D19 S25.

Hansen, A.D.A., Conway, T.J., Steele, L.P., Bodhaine, B.A., Thoning, K.W., Tans, P., Novakov, T., 1989. Correlations among combustion effluent species at Barrow, Alaska: aerosol black carbon, carbon dioxide, and methane. Journal of Atmospheric Chemistry 9, 283–299.

Heald, C.L., et al., 2003. Asian outflow and trans Pacific transport of carbon monoxide and ozone pollution: an integrated satellite, aircraft, and model perspective. Journal of Geophysical Research 108, 4804.

Heald, C.L., Jacob, D.J., Jones, D.B.A., Palmer, P.I., Logan, J.A., Streets, D.G., Sachse, G.W., Gille, J.C., Hoffman, R.N., Nehrkorn, T., 2004. Comparative inverse analysis of satellite (MOPITT) and aircraft (TRACE-P) observations to estimate Asian sources of carbon monoxide. Journal of Geophysical Research 109 (D23), D23306.

Jaffe, D.A., Honrath, R.E., Furness, D., Conway, T.J., Dlugokencky, E., Steele, L.P., 1995. An estimate of the CH_4, NO_x, and CO_2 emissions from the Prudhoe Bay, Alaska, oil development. Atmospheric Chemistry 20, 213–227.

Jaffe, D.A., Anderson, T., Covert, D., Kotchenruther, R., Trost, B., Danielson, J., Simpson, W., Berntsen, T., Karlsdottir, S., Blake, D., Harris, J., Carmichael, G., Uno, I., 1999. Transport of Asian air pollution to North America. Geophysical Research Letters 26, 711–714.

Jaffe, D.A., Anderson, T., Covert, D., Trost, B., Danielson, J., Simpson, W., Blake, D., Harris, J., Streetss, D., 2001. Observations of ozone and related species in the Northeast Pacific during the PHOBEA campaigns: 1. Ground based observations at Cheeka Peak. Journal of Geophysical Research 106, 7449–7461.

Jaffe, D.A., McKendry, I., Anderson, T., Price, H., 2003. Six 'new' episodes of trans-Pacific transport of air pollutants. Atmospheric Environment 37, 391–404.

Kanaya, Y., et al., 2001. Behavior of OH and HO2 radicals during the observations at a remote Island of okinawa (ORION99) field campaign 1. Observation during a laser-induced fluorescence instrument. Journal of Geophysical Research 106, 24,197–24,208.

Kasibhatla, P., Arellano, A., Logan, J.A., Palmer, P.I., Novelli, P., 2002. Top-down estimate of a large source of atmospheric carbon monoxide associated with fuel combustion in Asia. Geophysical Research Letters 29.

Kato, S., et al., 2004. Transport of atmospheric carbon monoxide, ozone, and hydrocarbons from Chinese coast to Okinawa island in the Western Pacific during winter. Atmospheric Environment 38, 2975–2981.

Kim, K.H., Kim, M.Y., 2000. The effects of anthropogenic sources on temporal distribution characteristics of total gaseous mercury in Korea. Atmospheric Environment 34, 3337–3347.

Kotchenruther, R.A., Jaffe, D.A., Beine, H.J., Anderson, T., Bottenheim, J.W., Harris, J.M., Blake, D., Schmitt, R., 2001. Observations of ozone and related species in the Northeast Pacific during the PHOBEA campaigns: 2. Airborne observations. Journal of Geophysical Research 106, 7463–7483.

Landis, M.S., Stevens, R.K., Schaedlich, F., Prestbo, E.M., 2002. Development and characterization of an annular denuder methodology for the measurement of divalent inorganic reactive gaseous mercury in ambient air. Environmental Science and Technology 36, 3000–3009.

Lin, C., Pehkonen, S.O., 1999. The chemistry of atmospheric mercury: a review. Atmospheric Environment 33, 2067–2079.

Mason, R.P., Fitzgerald, W.F., Morel, F.M.M., 1994. The biogeochemical cycling of elemental mercury: anthropogenic influences. Geochimica Cosmochimica Acta 58, 3191–3198.

Mukherjee, A.B., Melanen, M., Ekqvist, M., Verta, M., 2000. Assessment of atmospheric mercury emissions in Finland. Science of the Total Environment 259, 73–83.

Pacyna, E.G., Pacyna, J.M., 2002. Global emission of mercury from anthropogenic sources in 1995. Water, Air and Soil Pollution 137, 149–165.

Pacyna, J.M., Pacyna, E.G., Steenhuisen, F., Wilson, S., 2003. Global mercury emissions. Presented at Long-Range Transport Workshop, Ann Arbor, MI, September 2003.

Palmer, P.I., Jacob, D.J., Jones, D.B.A., Heald, C.L., Yantosca, R.M., Logan, J.A., Sachse, G.W., Streets, D.G., 2003. Inverting for emissions of carbon monoxide from Asia using aircraft observations over the western Pacific. Journal of Geophysical Research 108.

Prestbo, E.M., Bloom, N.S., 1995. Mercury speciation adsorption (MESA) method for combustion flue gas: methodology, artifacts, intercomparison and atmospheric implications. Water, Air and Soil Pollution 80, 145.

Prestbo, E.M., Swartzendruber, P., Levin, L., Aljoe, W., Jansen, J., Monroe, L., Michaud, D., Laudal, D., Schulz, R., Dunham, G., Valente, R., 2004. Interconversion of emitted atmospheric mercury species in coal-fired power plant plumes. Proceedings of the Seventh International Conference on Mercury as a Global Pollutant, Ljubljana, Slovenia, June 2004.

Price, H.U., Jaffe, D.A., Cooper, O.R., Doskey, P.V., 2004. Photochemistry, ozone production, and dilution during long-range transport episodes from Eurasia to the northwest United States. Journal of Geophysical Research 109, D23S13.

Schroeder, W.H., Munthe, J., 1998. Atmospheric mercury—an overview. Atmospheric Environment 32, 809–822.

Schroeder, W.H., Anlauf, K.G., Barrie, L.A., Lu, J.Y., Steffen, A., Schneeberger, D.R., Berg, T., 1998. Arctic springtime depletion of mercury. Nature 394, 331–332.

Schuster, P.F., Krabbenhoft, D.P., Naftz, D.L., Cecil, L.D., Olson, M.L., Dewild, J.F., Susong, D.D., Green, J.R., Abbott, M.L., 2002. Atmospheric mercury deposition during the last 270 years: a glacial ice core record of natural and anthropogenic sources. Environmental Science and Technology 36, 2303–2310.

Seigneur, C., Vijayaraghavan, K., Lohman, K., Karamchandani, P., Scott, C., 2004. Global source attribution for mercury deposition in the United States. Environmental Science and Technology 38, 555–569.

Slemr, F., Langer, E., 1992. Increase in global atmospheric concentrations of mercury inferred from measurements over the Atlantic Ocean. Nature 355, 434–437.

Tan, H., He, J.L., Liang, L., Lazoff, S., Sommer, J., Xiao, Z.F., Lindqvist, O., 2000. Atmospheric mercury deposition in Guizhou, China. Science of the Total Environment 259, 223–230.

US EPA, 1997. Mercury Study Report to Congress, EPA-452-R-97-004.

US EPA, 2000. National Air Pollutant Emission Trends, 1900–1998, EPA-454/R-00-002, March 2000.

Weiss-Penzias, P., Jaffe, D.A., McClintick, A., Prestbo, E.M., Landis, M.S., 2003. Gaseous elemental mercury in the marine boundary layer: evidence for rapid removal in anthropogenic pollution. Environmental Science and Technology 37 (17), 3755–3763.

Weiss-Penzias, P., Jaffe, D.A., Jaeglé, L., Liang, Q., 2004. Influence of long-range-transported pollution on the annual and diurnal cycles of carbon monoxide and ozone at Cheeka Peak Observatory. Journal of Geophysical Research 109, D23S14.